DØ note # 2963
June 1, 1996

Determinations of the Mass of the Top Quark Using the Topological Variables

Frank Hsieh, Jianming Qian
Department of Physics
The University of Michigan
Ann Arbor, Michigan 48109

ABSTRACT

The distributions of topological variables of $t\bar{t}$ events depend on the mass of the top quark. By comparing the measured distributions of the $t\bar{t}$ candidate events with those expected from the $t\bar{t}$ and the background events, the top quark mass can be inferred. In this note, we present an analysis using three topological variables: transverse energy (H_T), transverse mass (M_T) and total mass (M) of the events. The top quark mass inferred from the distributions of these variables of the 34 lepton+jets candidate events are consistent with that determined using the kinematically constrained fit. Among the three distributions, the distribution of the H_T variable is the least susceptible to systematic uncertainties. The top quark mass extracted from the H_T distribution is $178 \pm 21(\text{stat}) \pm 10(\text{syst})$ GeV/c^2 for the background constrained fit and is $170 \pm 18(\text{stat}) \pm 10(\text{syst})$ GeV/c^2 for the background unconstrained fit. The fitted distributions describe the distributions of the candidate events well.

1 Introduction

In a lepton+jets $t\bar{t}$ candidate event, one expects to have four jets (two b–quark jets and two light–quark jets), one isolated high p_T lepton and large missing E_T. Moreover, the events are expected to satisfy several kinematic constraints. By utilizing these constraints, the mass of the top quark can be determined. The analysis starts with two–constraint kinematic fits of candidate events to the hypothesis $t\bar{t} \to W^+W^-b\bar{b} \to \ell\nu q\bar{q}b\bar{b}$ using the measured quantities of jets, leptons and the missing transverse momentum, resulting in a distribution of the fitted mass for the candidate events. The top quark mass is then extracted by comparing the distribution of the fitted mass of the candidate events with those expected from $t\bar{t}$ and background events. Details of this method can be found in [1].

In this note, we present a complementary analysis of the top quark mass. Instead of employing the kinematic constraints which require the jet energies be corrected back to the parton level, the method described below utilizes the mass dependences of the topological distributions of the $t\bar{t}$ events. The top quark mass is inferred by comparing the topological distributions of candidate events with those expected from $t\bar{t}$ and background events, side–stepping the complicated correction procedure for the jet energies.

The approach of the kinematically constrained fit has been investigated extensively in DØ. The mass of the top quark has been measured to be $170 \pm 15(\text{stat}) \pm 10(\text{syst})$ GeV/c^2 [2] using this method. The approach using topological variables has been largely ignored. In this note, we present a top quark mass analysis using the distributions of three topological variables: transverse energy (H_T), transverse mass (M_T) and total mass (M) of the $t\bar{t}$ candidate events to complement the first approach. We note that the two methods are in principle very similar. In fact, the fitted mass is just one of many topological variables. Unlike the above three topological variables which can be calculated straightforwardly from the measured quantities of the candidate event, the fitted mass has to be extracted from a complicated fitting procedure. Moreover, these two approaches are subject to different systematic effects. While the distribution of the fitted mass is broadened by the combinatoric backgrounds, the distributions of the topological variables are often smeared by the transverse and longitudinal boosts of the top quark. Finally, we point out that by comparing the topological distributions of the candidate events with those expected from the $t\bar{t}$ events, we are implicitly testing the kinematics of the candidate events.

2 Data and Monte Carlo Samples

The lepton+jets $t\bar{t}$ candidate events used in this analysis are selected using the 'New Loose' selection criteria from an integrated luminosity of about 100 pb^{-1} recorded in Run IA and IB. A total of 34 lepton+jets candidate events (14 e+jets, 4 e+jets/μ, 14 μ+jets, 2 μ+jets/μ) is selected with an estimated 19.6 ± 2.6 background events. The background is dominated by the W+jets events which accounts for 83% of the total background. The remaining 17% is from the QCD multijet events. The selection criteria is described in [2].

For the analysis described below, W+jets background is modeled using VECBOS [5] Monte Carlo program and the QCD multijet background is modeled using data with fake leptons. The $t\bar{t}$ events are primarily modeled using HERWIG 5.7 [3] event generator with 9 different values of the top quark mass ranging from 140 to 240 GeV/c^2. For comparisons, the analysis is repeated using the ISAJET 7.13 event generator.

The events used in this analysis are reconstructed using RECO version 11 or higher and CAFIX 5.0. Unlike the kinematically constrained fit for which the jet energies must be corrected back to those of the corresponding partons, the jet energies for this analysis are not corrected for the out–of–cone gluon radiations.

3 Topological Variables

The topological variables studied in this analysis are the transverse energy (H_T), the transverse mass (M_T) and the total mass (M). They are calculated using the measured quantities of jets, high p_T electrons and muons as defined below:

$$H_T = \sum_{j,\ell} E_T$$

$$M_T = \sqrt{(\sum_{j,\ell} \sqrt{p_x^2 + p_y^2})^2 - (\sum_{j,\ell} p_x)^2 - (\sum_{j,\ell} p_y)^2}$$

$$M = \sqrt{(\sum_{j,\ell} E)^2 - (\sum_{j,\ell} p_x)^2 - (\sum_{j,\ell} p_y)^2 - (\sum_{j,\ell} p_z)^2}$$

where the $\sum_{j,\ell}$ sums over all jets with $E_T > 15$ GeV and $|\eta| < 2.0$, isolated electrons with $E_T > 20$ GeV and $|\eta| < 2.0$ and isolated muons with $E_T > 20$ GeV and $|\eta| < 1.7$. The jets reconstructed with a R=0.5 cone algorithm are used in the analysis. It should be noted that strong correlations exist among these variables.

The H_T, M_T and M distributions of the HERWIG 5.7 $t\bar{t}$ events for four different masses of the top quark are shown in Fig. 1. The distributions strongly depend on the top quark mass (m_t). As m_t increases, the topological distributions are shifted toward high values of the variables. The correlations are characterized in Fig. 2 using the mean values of the distributions and are well described by the linear fits $< V >= am_t + b$. The slopes from the fits are 1.30, 1.29 and 1.59 for the H_T, M_T and M respectively. The sensitivities to the top quark mass are largely determined by the two parameters: the slope of the correlation and the width of the distribution. The sensitivity to m_t for different variables can be compared using the parameter:

$$S \equiv \frac{\sigma(m_t)}{a}$$

where $\sigma(m_t)$ is the root–mean–square of the distribution and a is the slope of the correlation. To a good approximation, the parameter S is the statistical error on the determined m_t for one candidate event for the case of zero–background event. For $m_t = 170$ GeV/c^2, the sensitivity parameter S are 57.3, 58.8 and 58.3 GeV for the H_T, M_T and M variables. Given the strong

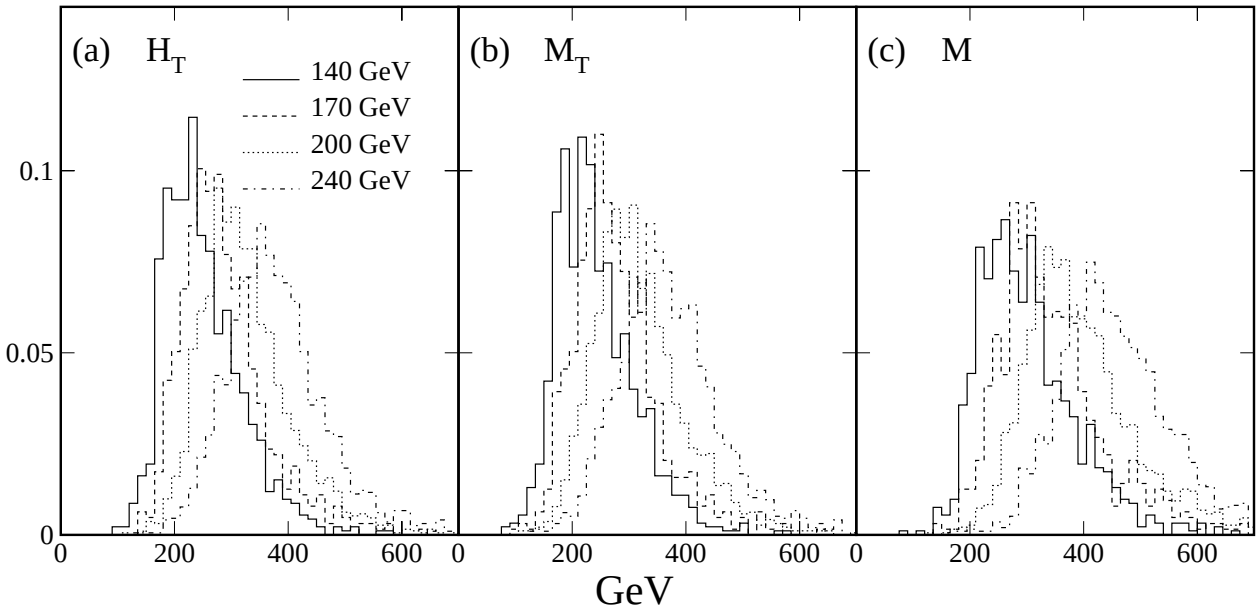

Figure 1: Topological distributions for the (a) H_T, (b) M_T and (c) M variables of the HERWIG 5.7 $t\bar{t}$ events for four different top quark masses. The distributions are normalized to the unit probability.

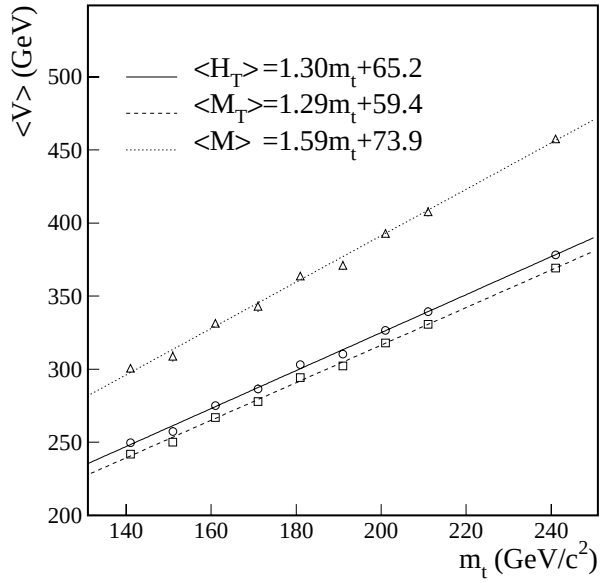

Figure 2: Correlations between the mean values of the three topological variables and the top quark mass for the HERWIG 5.7 $t\bar{t}$ events. The lines are linear fits to the respective Monte Carlo data points.

correlations among the three variables, it is not surprising that these variables are equally sensitive to m_t. In fact, the H_T and M_T distributions are very similar, as shown in the Fig. 1 and 2. Finally, we note that including missing E_T in the H_T and M_T calculations increases the slopes of the correlations. However, the sensitivity parameters S are essentially unchanged due to the increased widths.

For comparisons, we note that the distribution of the fitted mass has a width 32 GeV for 170 GeV/c^2 top quark and a slope of 0.72 for the correlation [6] between the mean value and the input mass, resulting in a sensitivity parameter of 44.4 GeV which is about 30% smaller than that of H_T. It suggests that the fitted mass is more sensitive to the m_t. This comes as no surprise. While the fitted mass is approximately Lorentz invariant, the H_T, M_T and M variables depend on the transverse momentum of the top quark. In the case of the M variable, the distribution is also convoluted by the longitudinal spectrum of the top quark. Consequently, the distributions of the topological variables are generally broader than that of the fitted mass, resulting in larger overlaps between the distributions of different masses of the top quark and reduced sensitivity to the m_t.

4 Fitting Procedure

To determine the mass of the top quark, the topological distributions of the 34 lepton+jets candidate events are fitted with the distributions of the $t\bar{t}$ and background events using an unbinned maximum likelihood method. For a topological variable V, a set of distributions of the HERWIG 5.7 $t\bar{t}$ Monte Carlo events with known top quark mass is used to interpolate the distribution for an arbitrary top quark mass. As shown in Fig. 1, the statistical fluctuations of the topological distributions are relatively large. This level of fluctuation not only makes the direct interpolation of the distributions unpractical, but also the maximum likelihood fit unsuitable. These distributions must be smoothed before the likelihood fit can proceed.

To reduce the fluctuations and to make the distributions interpolatable, we introduce a scaled variable x for each topological variable V ($V = H_T, M_T, M$):

$$x \equiv \frac{V - < V > (m_t)}{\sigma(m_t)}$$

where $< V > (m_t)$ and $\sigma(m_t)$ are the mean value and the width (root–mean–square) of the distribution of the $t\bar{t}$ events with a top quark mass m_t respectively. The probability functions $f(x, m_t)$, normalized to the unit sum of the contents, for the variable x for four different values of m_t are compared in Figs. 3(a-c) for the H_T, M_T and M variables. As evident from the figures, the functions $f(x, m_t)$ of each variable for the different top quark masses agree within the statistics, almost independent of m_t. This observation leads us to add the $f(x, m_t)$ functions for different mass of the top quark together to reduce the statistical fluctuations, resulting in a higher statistics probability function $f(x)$.

Once the probability function $f(x)$ for the scaled variable x is determined and smoothed, only the mean value $< V > (m_t)$ and the width $\sigma(m_t)$ are need to be interpolated to yield a probability function $g(V, m_t)$ for the topological variable V given an arbitrary value of m_t. As

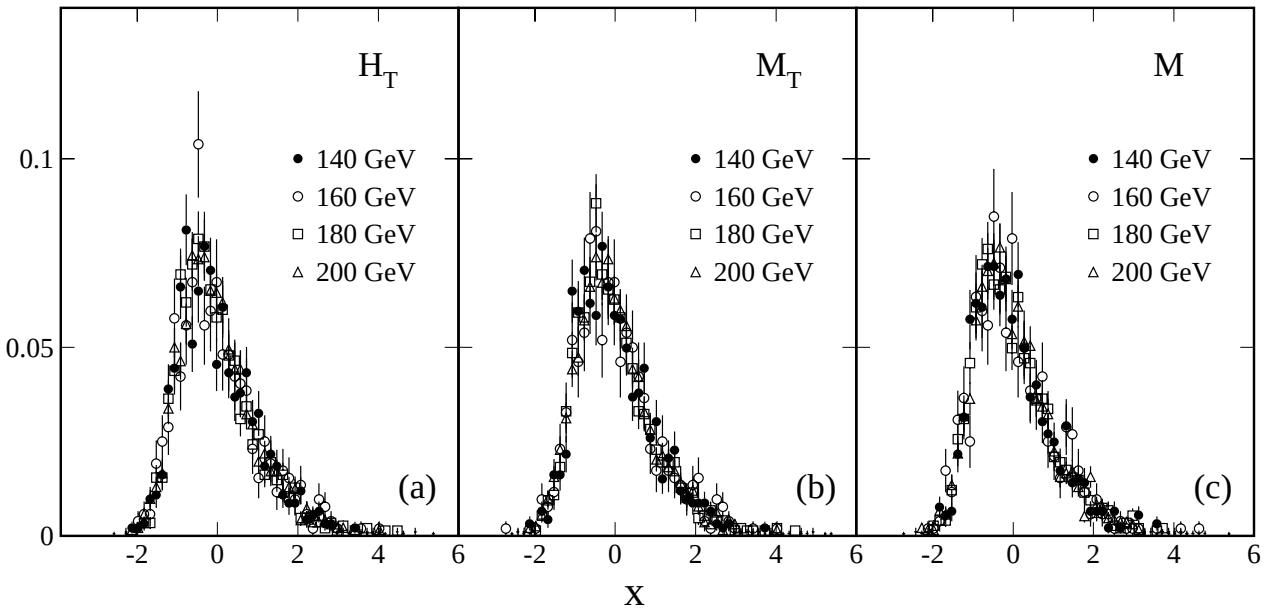

Figure 3: Comparisons of the probability functions $f(x, m_t)$ for four different values of m_t for the H_T, M_T and M variables. The functions are normalized to have unit sums of the contents. The $f(x, m_t)$ functions of each variable agree within the statistics for different values of m_t.

Variables		m_t (GeV/c^2)									Bkgd
Mean & Width		140	150	160	170	180	190	200	210	240	
H_T	$< H_T >$	249.7	257.3	275.0	286.4	303.1	310.4	326.6	339.3	378.2	222.6
(GeV)	σ	68.0	63.2	73.3	74.5	80.1	71.5	80.6	78.1	86.0	82.4
M_T	$< M_T >$	241.9	250.2	267.0	277.9	294.1	302.3	318.0	330.7	369.2	214.1
(GeV)	σ	68.9	64.5	74.3	75.9	81.3	73.4	81.5	80.2	87.7	78.8
M	$< M >$	300.6	308.7	331.3	342.9	363.7	371.0	393.3	407.7	457.6	270.8
(GeV)	σ	86.4	78.6	90.9	92.7	95.8	91.0	98.7	91.9	100.2	101.8

Table 1: The mean values and the widths of the three topological variables of the HERWIG 5.7 $t\bar{t}$ events for 9 different values of the top quark mass and of the background events.

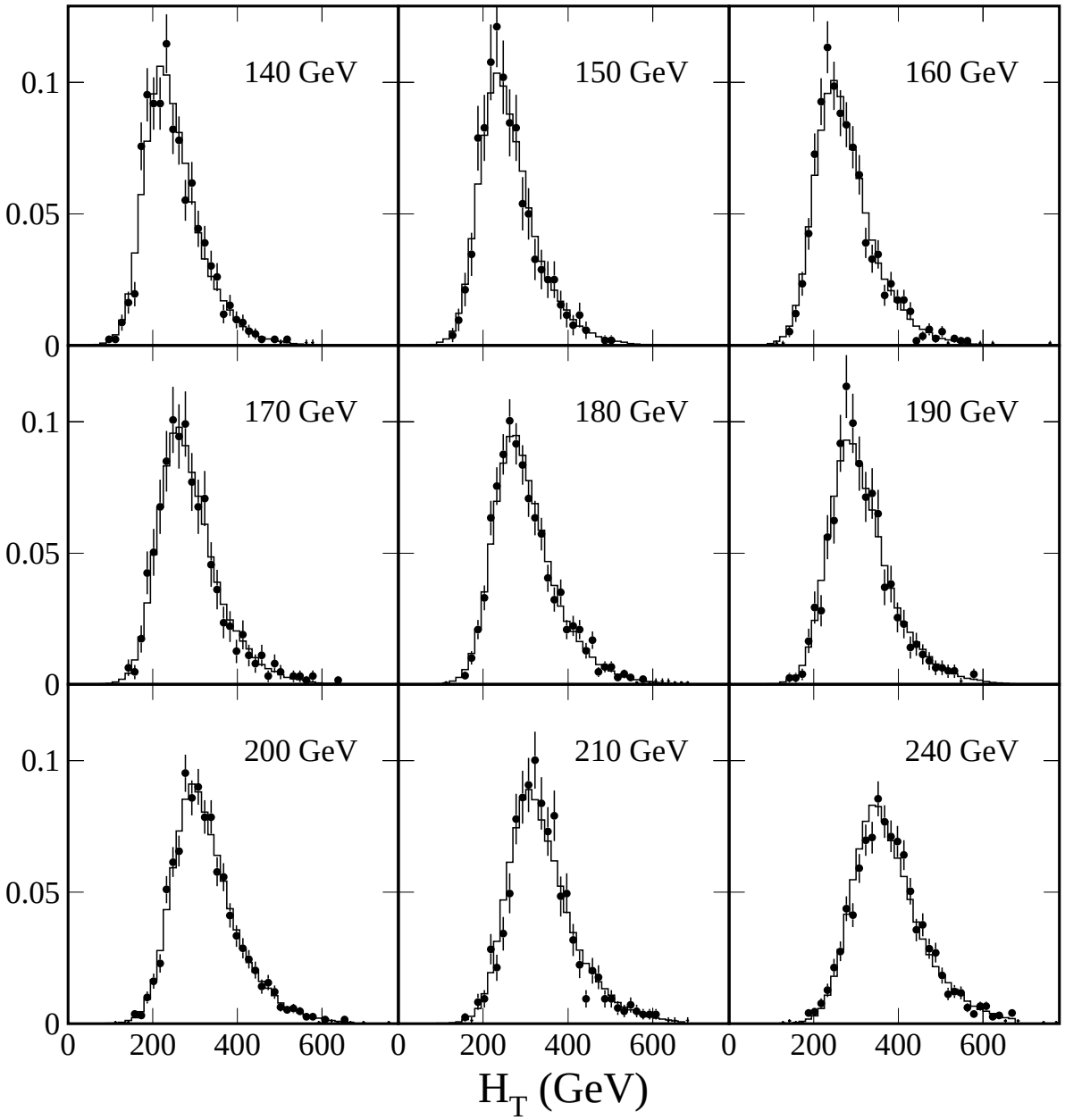

Figure 4: The H_T distributions of the HERWIG 5.7 $t\bar{t}$ events before (dots) and after (histograms) interpolation for 9 different top quark masses. The interpolated distributions reproduce the original distributions well. All distributions are normalized to the unit probability. The probabilities that the distributions before and after interpolation arise from the same parent distributions are estimated to be 0.72, 0.44, 0.71, 0.97, 0.73, 0.55, 1.00, 0.56 and 0.12 respectively for the 9 distributions.

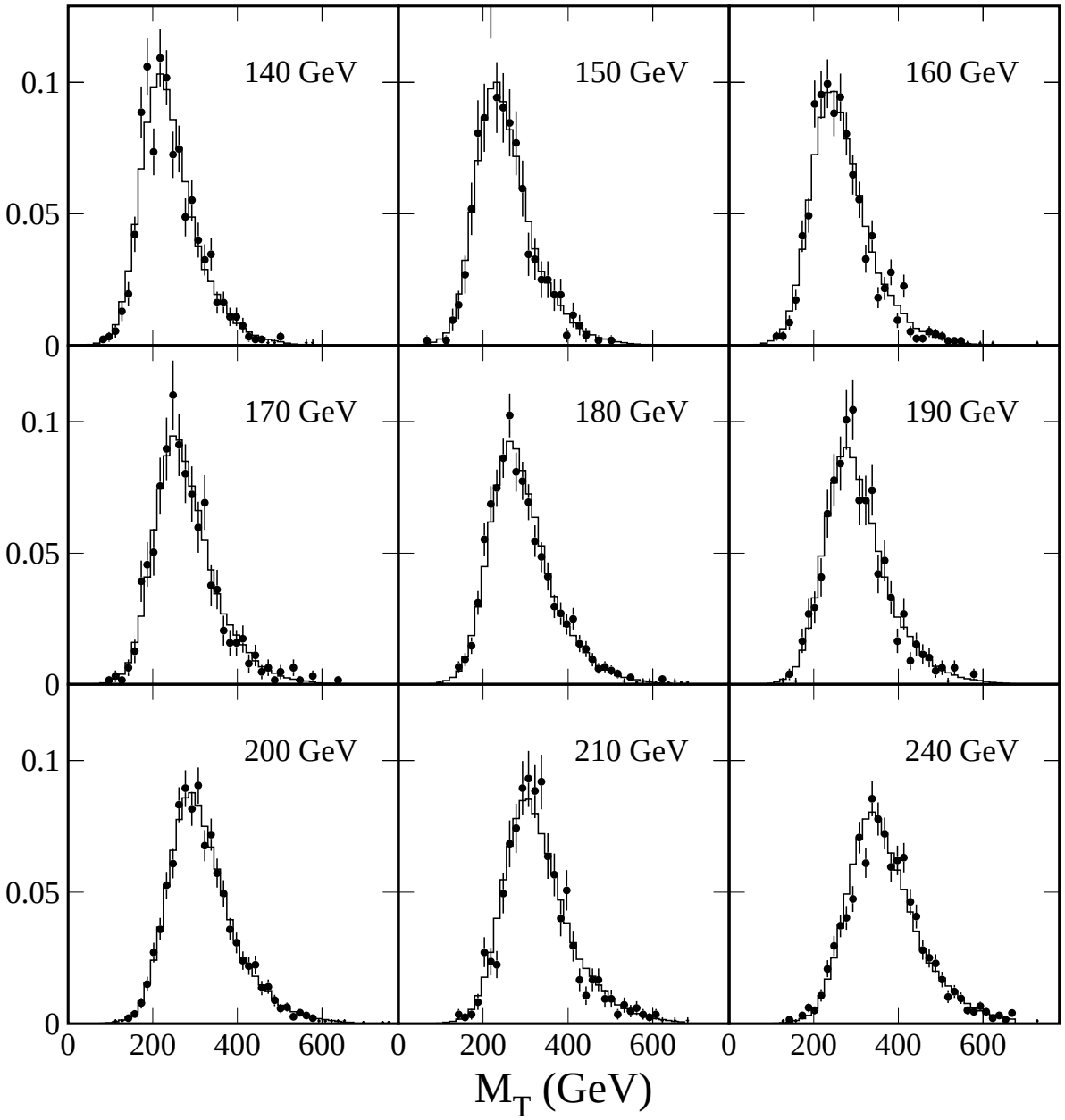

Figure 5: The M_T distributions of the HERWIG 5.7 $t\bar{t}$ events before (dots) and after (histograms) interpolation for 9 different top quark masses. The interpolated distributions reproduce the original distributions well. All distributions are normalized to the unit probability. The probabilities that the distributions before and after interpolation arise from the same parent distributions are estimated to be 0.71, 0.67, 0.92, 0.92, 0.65, 0.80, 1.00, 0.70 and 0.18 respectively.

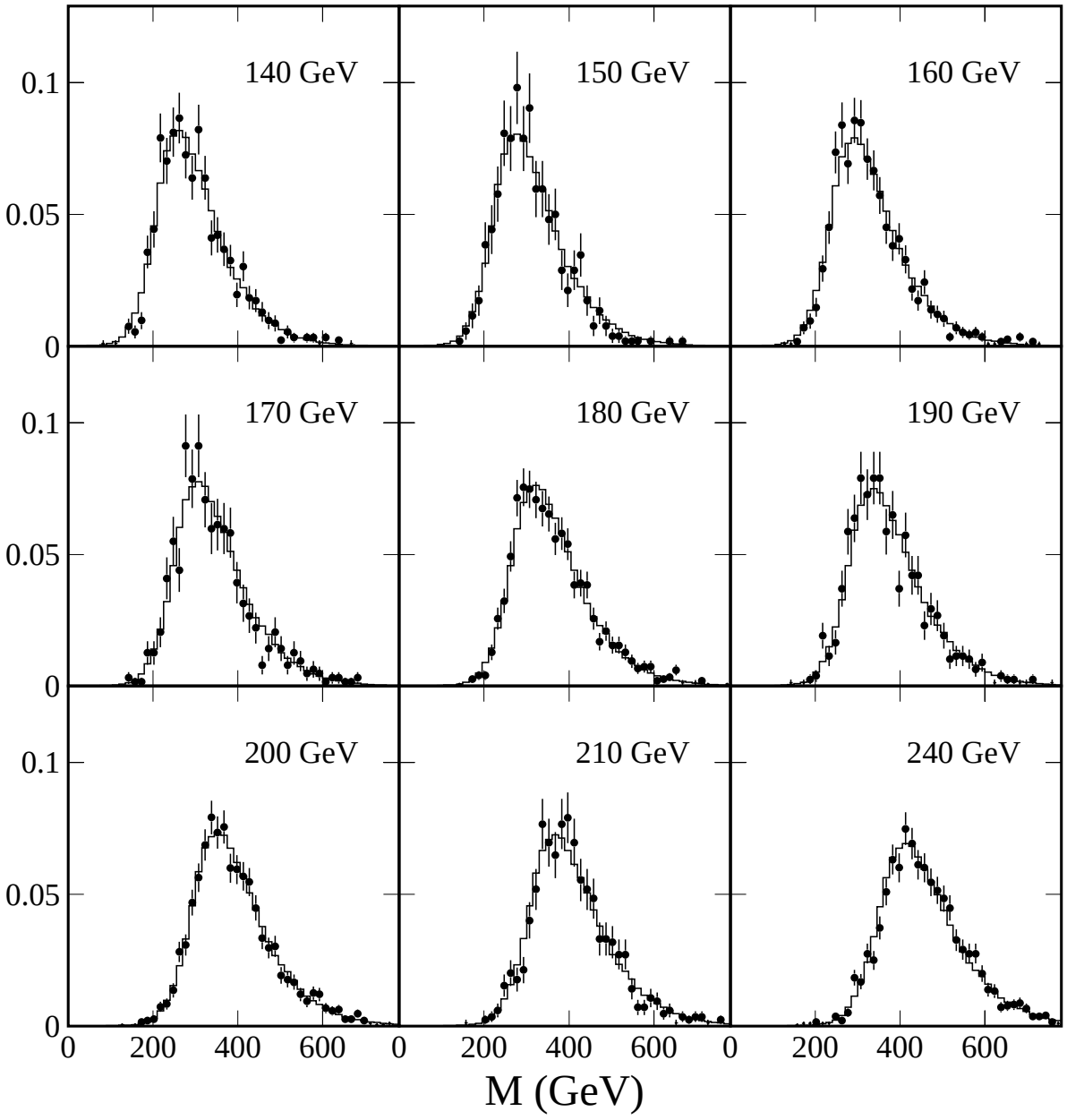

Figure 6: The M distributions of the HERWIG 5.7 $t\bar{t}$ events before (dots) and after (histograms) interpolation for 9 different top quark masses. The interpolated distributions reproduce the original distributions well. All distributions are normalized to the unit probability. The probabilities that the distributions before and after interpolation arise from the same parent distributions are estimated to be 0.74, 0.58, 0.73, 0.36, 0.90, 0.19, 0.95, 0.79 and 0.37 respectively.

shown in Fig. 2, the correlations between the mean value and the top quark mass are adequately described by linear functions. As shown in Table 1, the width of the distributions also increases with m_t although the fluctuations are relatively large. For simplicity, a linear approximation is used for the correlation between the width and the mass. Therefore, the interpolations of the complicated distributions are reduced to the linear interpolations of the mean values and the widths of the distributions. The topological distributions before and after interpolation are compared in Figs. 4–6 for the H_T, M_T and M variables for 9 different values of the top quark mass for the HERWIG 5.7 $t\bar{t}$ events. The interpolated distributions are smooth and they reproduce the uninterpolated Monte Carlo distributions well. The estimated probabilities[1] that the distributions before and after the interpolations arise from the same parent distribution are very high and are above 50% for most of the distributions.

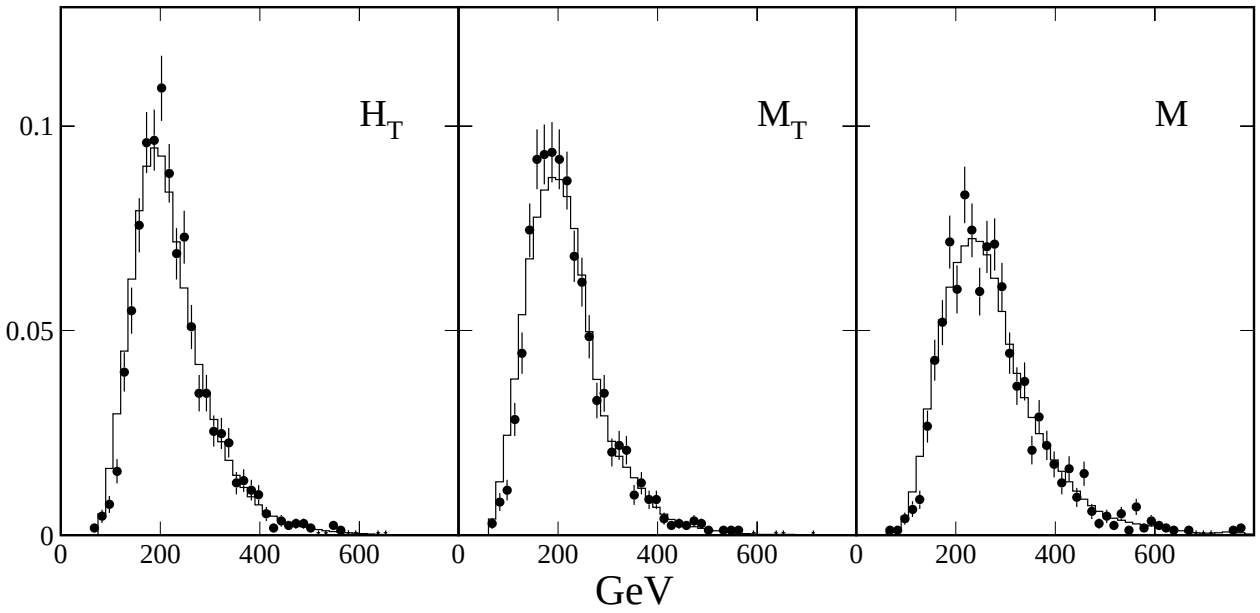

Figure 7: The background distributions for the H_T, M_T and M variables together with their smoothed distributions used in the fits, assuming a background mixture of 83% of W+jets and 17% of QCD multijets events. All distributions are normalized to the unit probability.

The background distributions are modeled using a mixture of 83% of W+jets and 17% of QCD multijet events. The VECBOS Monte Carlo is used to generate W+jets distribution while the data with fake leptons are used for the QCD multijet distribution. The resulting background distributions are shown in Fig. 7 for the three variables together with their smoothed distributions. The mean values and the widths are listed in Table 1.

To extract the mass of the top quark, the following likelihood function is maximized by varying the mass of the top quark m_t, the number of the expected $t\bar{t}$ events n_s and the number

[1]The probabilities are estimated using the PAW command HIST/OPER/DIFF.

of the expected background events n_b:

$$\mathcal{L}(m_t, n_s, n_b) = \frac{e^{-(n_s+n_b)}}{N!}(n_s+n_b)^N \cdot e^{-\frac{(n_b-<n_b>)^2}{2\sigma_b^2}} \cdot \prod_i \frac{n_s g_s(V_i, m_t) + n_b g_b(V_i)}{n_s + n_b}$$

where N is the total number of candidate events, $< n_b >$ and σ_b are the estimated number of background events and its error, $g_s(V_i, m_t)$ and $g_b(V_i)$ are the probability functions for the $t\bar{t}$ and background events. The first term of the likelihood function represents the Poisson statistics while the second term constrains the number of background events. The last term is a product of the event probabilities. The product $\prod_i$ runs over all candidate events. For the background unconstrained fits, the second term is dropped.

5 Fitting Results

Two fits are performed for each variable, one with the number of background events (n_b) constrained within its error to 19.6 ± 2.6, the other with the number of background events unconstrained. The candidate and fitted topological distributions are shown in Fig. 8 for the background constrained fits and in Fig. 9 for the background unconstrained fits with the the $t\bar{t}$ distributions modeled by the HERWIG 5.7 program. The corresponding negative logarithmic likelihoods ($-\ln\mathcal{L}$) as functions of m_t are also presented in the same figures. The m_t and the numbers of the $t\bar{t}$ and the background events from the fits are shown in Table 2. The errors on the extracted masses are derived from the $-\ln\mathcal{L}$ functions with other fitting parameters fixed to their central values and are for reference only. The average H_T, M_T and M values of the candidate events are 265.1, 256.3 and 313.2 GeV respectively. The corresponding widths are 78.7, 80.5 and 88.6 GeV. As shown in the table, the sum of the numbers of the $t\bar{t}$ and the background events are greater than the number of the observed candidate events for all three variables, indicating that the fits prefer more $t\bar{t}$ events than the total number of observed events would allow. This fact is clearly manifested when the number of the background events is unconstrained. The background unconstrained fits generally yield smaller values of $-\ln\mathcal{L}$ (by approximately 0.5 unit) and prefer smaller numbers of background events over the background constrained fits. Consequently, more candidate events are assigned to the $t\bar{t}$ production in the background unconstrained fits, resulting in lower values of the extracted masses and smaller statistical errors on the masses. Finally, it is worth to point out that the fits to the H_T distribution have the smallest values of $-\ln\mathcal{L}$ among the three variables. Both background constrained and unconstrained fits describe the candidate distributions well.

Using the ISAJET 7.13 program to model the $t\bar{t}$ distributions generally results in slightly lower values of m_t for all three distributions. The differences can be traced to the differences in the topological distributions between the ISAJET 7.13 and HERWIG 5.7 $t\bar{t}$ events. As shown in Fig. 10(a) for $m_t = 170$ GeV/c^2, the H_T spectrum of the ISAJET 7.13 $t\bar{t}$ events is harder and broader than that of the HERWIG 5.7 program. The mean values of the H_T distribution as functions of m_t for the HERWIG 5.7 and ISAJET 7.13 $t\bar{t}$ events are compared in Fig. 10(b). The ISAJET 7.13 curve is systematically above that of the HERWIG 5.7 curve. Similar differences as shown in Table 1 for the HERWIG 5.7 and in Table 3 for the ISAJET 7.13 are seen for the M_T and M distributions. The results from the likelihood fits are shown in Table 4. The candidate

Variable	Background constrained			Background unconstrained		
	m_t (GeV/c^2)	n_s	n_b	m_t (GeV/c^2)	n_s	n_b
H_T	178 ± 16	17.1	18.9	170 ± 13	20.9	13.3
M_T	182 ± 20	16.7	19.0	171 ± 15	21.5	12.8
M	169 ± 12	17.8	18.7	163 ± 10	24.6	9.6

Table 2: The top quark masses from the likelihood fits to the three topological distributions of the 34 lepton+jets candidate events. The HERWIG 5.7 event generator is used to model the $t\bar{t}$ distributions. Also shown are the numbers of the $t\bar{t}$ and the background events from the fits. The errors on the extracted masses are determined from the likelihood functions with the other fitting parameters fixed to their central values. They are for reference only.

Variables		m_t (GeV/c^2)						Bkgd
Mean & Width		140	160	170	180	190	200	
H_T	$< H_T >$	259.4	282.6	299.3	313.3	323.5	332.0	222.6
(GeV)	σ	77.7	80.0	84.1	85.2	85.2	84.1	82.4
M_T	$< M_T >$	251.1	274.2	291.2	305.3	315.1	323.3	214.1
(GeV)	σ	75.9	80.7	84.9	86.6	86.4	85.6	78.8
M	$< M >$	309.5	338.8	361.2	377.8	390.5	399.4	270.8
(GeV)	σ	92.9	99.4	104.6	106.1	105.3	103.1	101.8

Table 3: The mean values and the widths of the three topological variables of the ISAJET 7.13 $t\bar{t}$ events for 6 different values of the top quark mass and of the background events.

Variable	Background constrained			Background unconstrained		
	m_t (GeV/c^2)	n_s	n_b	m_t (GeV/c^2)	n_s	n_b
H_T	175 ± 19	16.9	19.0	167 ± 22	21.3	13.0
M_T	174 ± 21	16.9	19.0	162 ± 18	22.5	11.8
M	163 ± 17	17.2	18.8	151 ± 10	27.0	7.2

Table 4: The top quark masses from the likelihood fits to the three topological distributions of the 34 lepton+jets candidate events. The ISAJET 7.13 event generator is used to model $t\bar{t}$ distributions. Also shown are the numbers of signal and background events from the fits. The errors on the extracted masses are determined from the likelihood functions with the other fitting parameters fixed to their central values. They are for reference only.

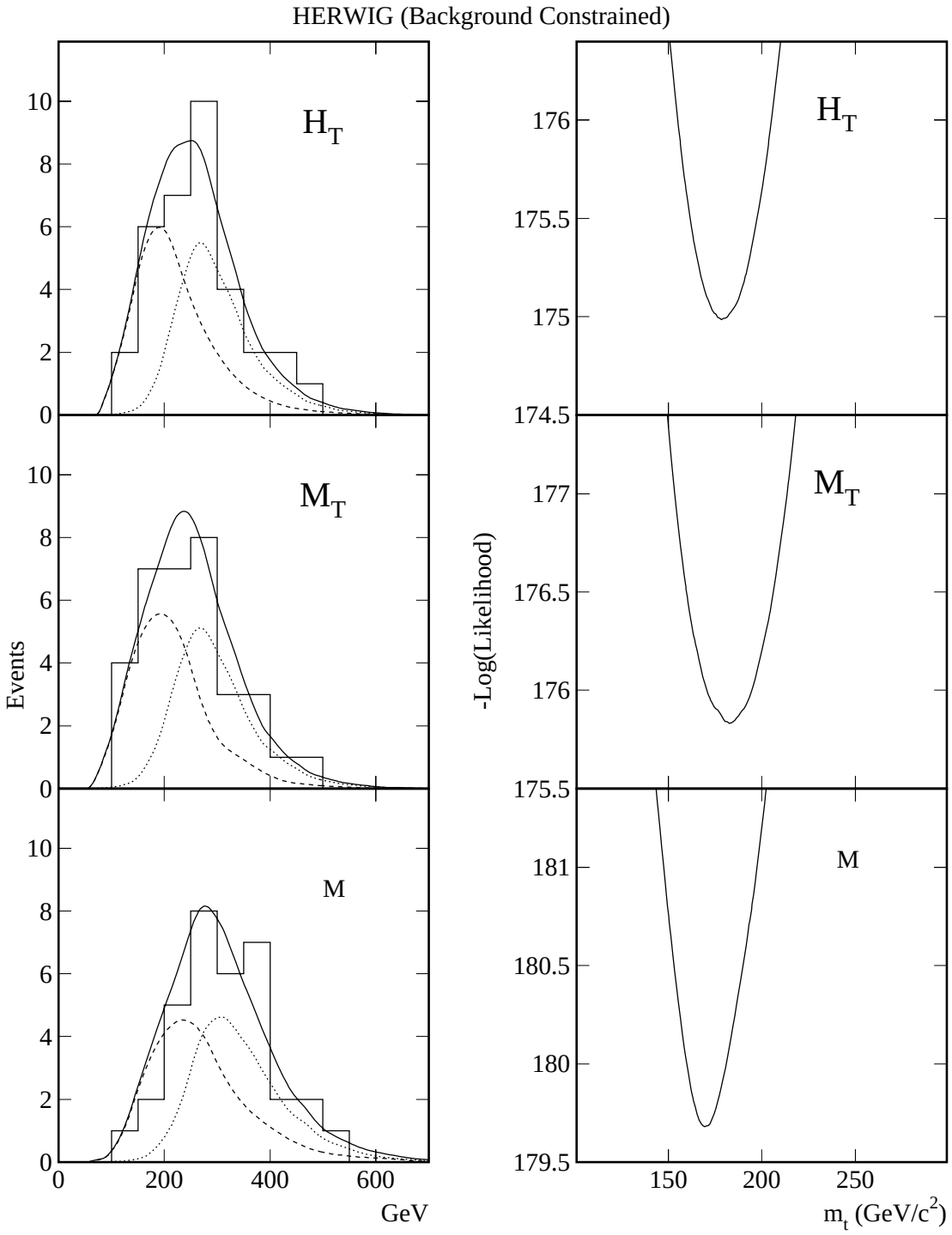

Figure 8: The background *constrained* fit using the HERWIG 5.7 program. Shown here are the topological distributions for candidate events (histograms) with the fitted distributions for $t\bar{t}$ events (dotted curves), background (dashed curves) and the sum of top and background (solid curves) for the H_T, M_T and M variables. The corresponding negative logarithmic likelihood functions are shown on the right. The number of background events is constrained to 19.6 ± 2.6 in the fits.

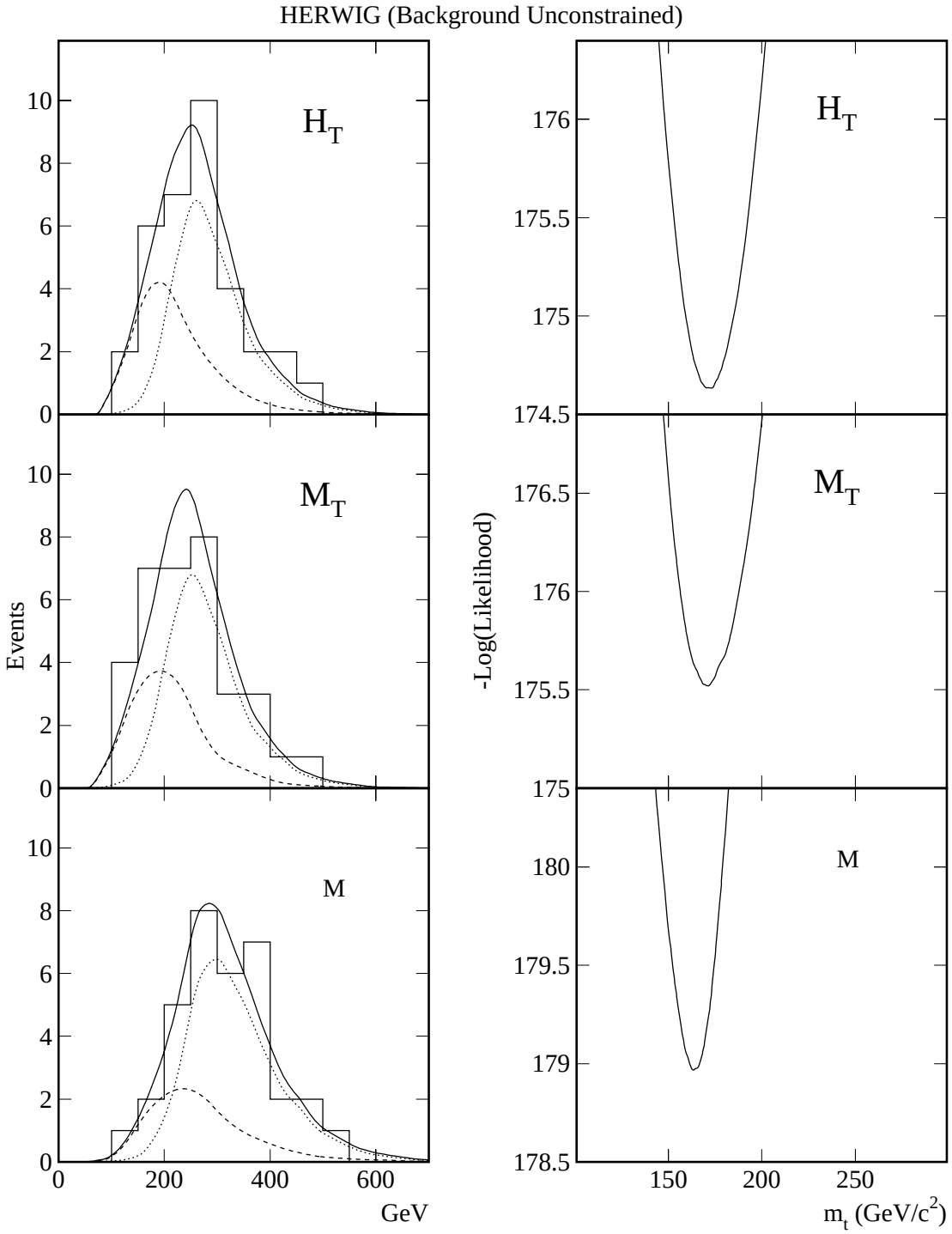

Figure 9: The background *unconstrained* fit using the HERWIG 5.7 program. Shown here are the topological distributions for candidate events (histograms) with the fitted distributions for $t\bar{t}$ events (dotted curves), background (dashed curves) and the sum of top and background (solid curves) for the H_T, M_T and M variables. The corresponding negative logarithmic likelihood functions are shown on the right.

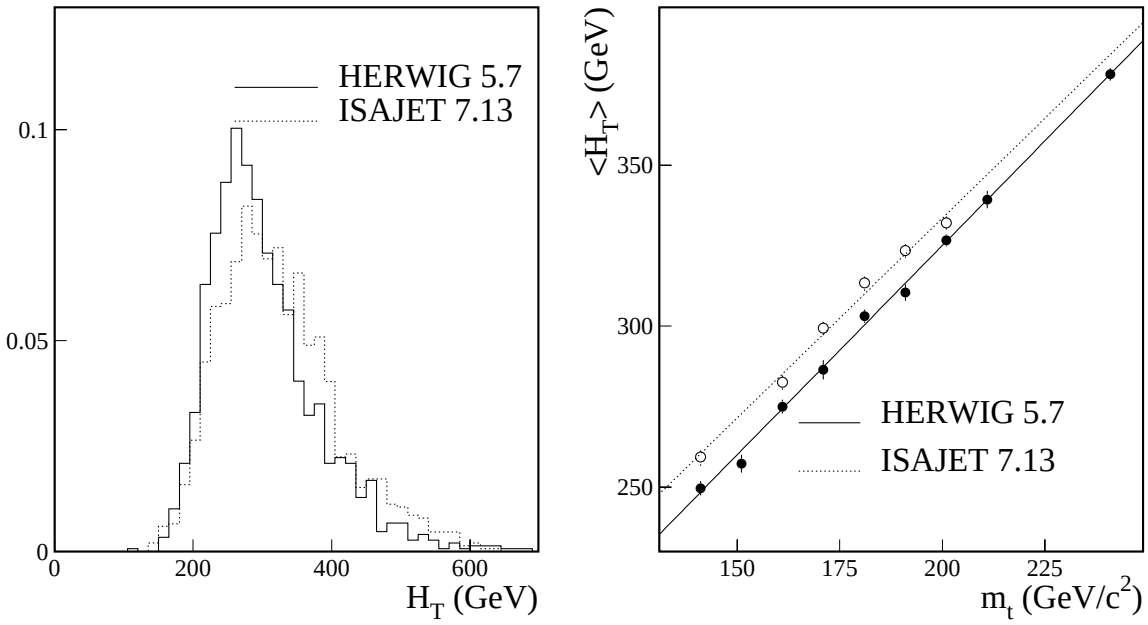

Figure 10: (a) The H_T distributions of the HERWIG 5.7 (solid histogram) and the ISAJET 7.13 (dotted histogram) $t\bar{t}$ events for a top quark mass of 170 GeV/c^2. (b) The mean value of H_T as functions of the top quark mass for the HERWIG 5.7 (solid circle) and the ISAJET 7.13 (open circle) $t\bar{t}$ events.

and fitted distributions are shown in Fig. 11 for the background constrained fits and in Fig. 12 for the background unconstrained fits. Similar to the HERWIG 5.7 model, the smaller number of background events are preferred by the background unconstrained fits, the total numbers of events from the background constrained fits exceed that of the observed events for all three variables and the fits to the H_T distribution have the smallest values of $-\ln\mathcal{L}$. As shown in the figures, the sums of the fitted ISAJET 7.13 and background distributions describe the distributions of candidate events well. Nevertheless, it is interesting to point out that the fit with HERWIG 5.7 model yields a smaller value of $-\ln\mathcal{L}$ than the fit with ISAJET 7.13 model for all three distributions. The differences in $-\ln\mathcal{L}$ are approximately 0.5 units for most cases.

6 Error Estimations

We estimate the statistical errors on the extracted m_t using Monte Carlo ensembles. These ensembles are subject to the same fitting procedure described above. For each ensemble, the numbers of the $t\bar{t}$ and the background events are allowed to fluctuate around the the central values of the corresponding fits to the 34 lepton+jets candidate events using the Poisson statistics. The background events are generated using the smoothed background distributions displayed in Fig. 7 and the $t\bar{t}$ distributions are simulated using the interpolated probability functions such as those shown in Fig. 4–6. As an example, Fig. 13(a) shows the m_t distribution extracted

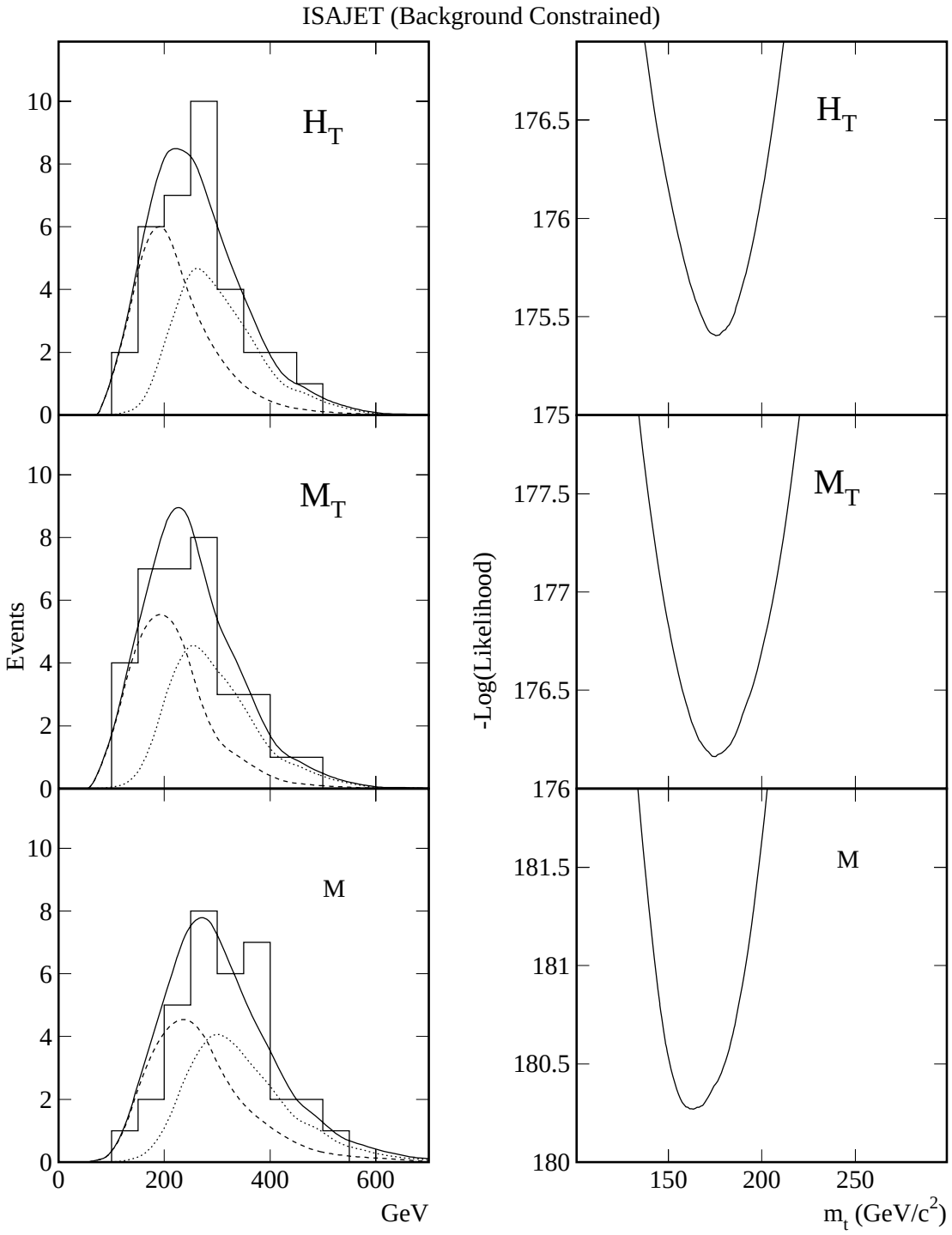

Figure 11: The background *constrained* fit using the ISAJET 7.13 program. Shown here are the topological distributions for candidate events (histograms) with the fitted distributions for $t\bar{t}$ events (dotted curves), background (dashed curves) and the sum of top and background (solid curves) for the H_T, M_T and M variables. The corresponding negative logarithmic likelihood functions are shown on the right. The number of background events is constrained to 19.6 ± 2.6 in the fits.

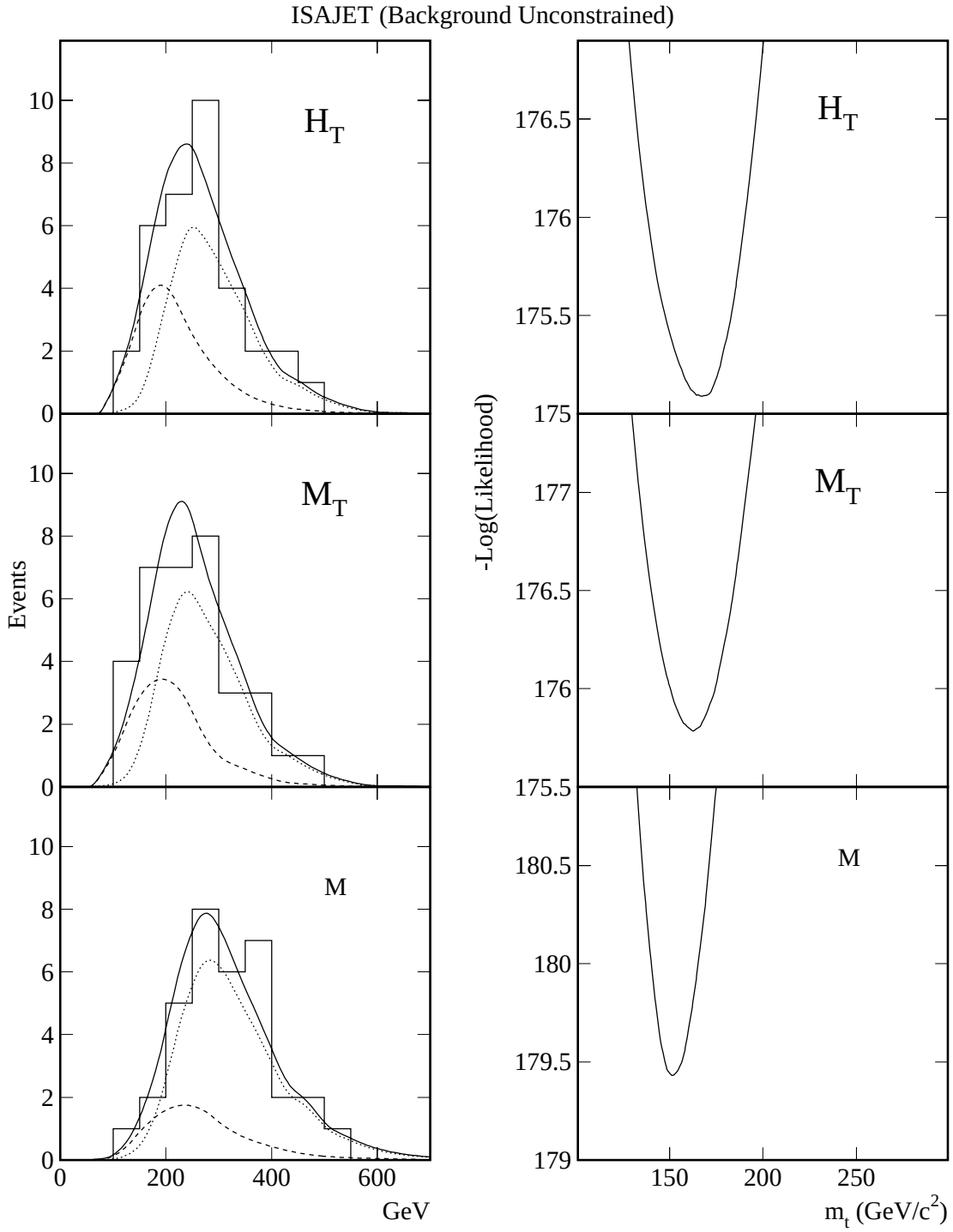

Figure 12: The background *unconstrained* fit using the ISAJET 7.13 program. Shown here are the topological distributions for candidate events (histograms) with the fitted distributions for $t\bar{t}$ events (dotted curves), background (dashed curves) and the sum of top and background (solid curves) for the H_T, M_T and M variables. The corresponding negative logarithmic likelihood functions are shown on the right.

from the background unconstrained fits to the H_T distributions of the 1,000 ensembles. These ensembles are generated with an input m_t of 170 GeV/c^2. The distribution has a mean of 170.7 GeV/c^2 and a width of 18.3 GeV/c^2. The widths of the distributions of the extracted mass from the ensembles are typically around 21 GeV/c^2 for the background constrained fits and are about 18 GeV/c^2 for the background unconstrained fits. These widths are assigned as the statistical errors on the extracted masses from the respective fits to the data.

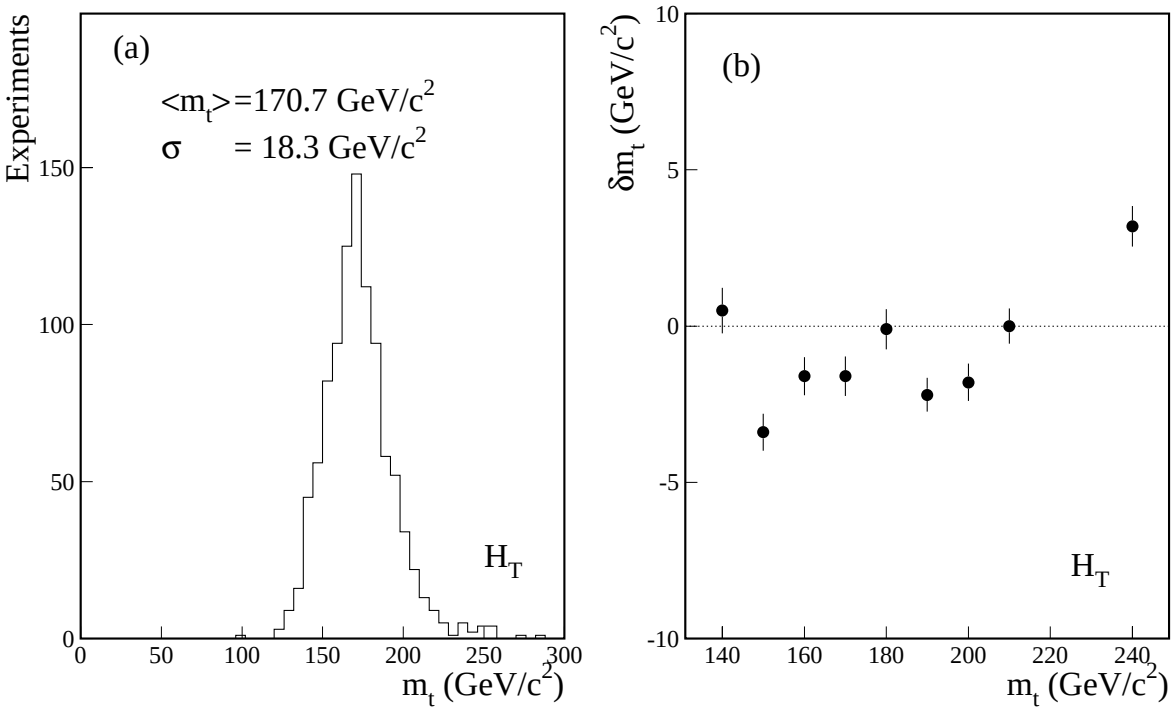

Figure 13: (a) The distribution of the top quark mass extracted from the background unconstrained fit to the H_T distributions of the 1000 ensembles with an input top quark mass of 170 GeV/c^2. The ensembles are generated using the smooth interpolated probability functions. (b) The differences between the mean values of the extracted top quark mass of the ensembles and the input top quark mass as functions of the input mass. The ensembles are generated using the uninterpolated probability functions. The fits are background constrained.

The uncertainty on the extracted mass due to the smoothing and the interpolation can be estimated by comparing the input mass of the top quark with the mean value of the distribution of the ensembles generated using the unsmoothed and uninterpolated probability functions of the $t\bar{t}$ and the background events. Fig. 13(b) shows the differences between the input masses and the mean values of the extracted mass as a function of the input mass for the background constrained fits. The largest difference, 3.4 GeV/c^2, is conservatively assigned as a systematic error. The results from the background unconstrained fits and for the other two variables are similar and are not repeated here.

The effect of the energy scale uncertainty is studied by repeating the fits to the observed 34 lepton+jets candidate events after rescaling the jet energies of the Monte Carlo HERWIG 5.7

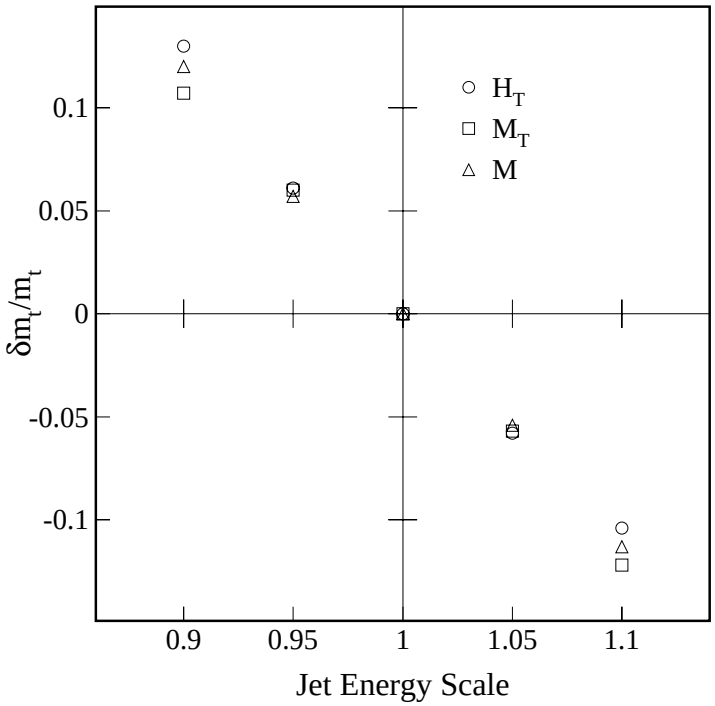

Figure 14: The variations of the top quark mass extracted from the background unconstrained fits to the data as functions of the jet energy scale for the three topological variables. The HERWIG 5.7 program events are used to modeled the $t\bar{t}$ distributions.

$t\bar{t}$ and VECBOS W+jets events. Fig. 14 shows the relative variations in the extracted mass for an energy scale ranging from 0.90 to 1.10 for the background constrained fits. The relative variations are approximately anti–correlated with the energy scale linearly. The results from the background unconstrained fits are very similar. For a 4% energy scale uncertainty quoted by the top mass group, the uncertainty on the extracted mass is approximately 4.5%.

Uncertainties in modelling the $t\bar{t}$ production and thereafter the probability functions of the $t\bar{t}$ events are another source of systematic error. For each variable, we average the difference in the extracted mass using the HERWIG 5.7 and ISAJET 7.13 models between the background constrained and unconstrained fits. The averaged difference which varies from 3 to 9 GeV/c^2 is assigned as a systematic error from the modelling for the variable. Finally, the uncertainties due to the shapes of the background distributions are studied by using distributions from 100% W+jets events and by using different smearing techniques. The studies show that the background unconstrained fits are more sensitive to the shapes of the background distributions than the background constrained fits. A difference as large as 4 GeV/c^2 in the extracted mass is observed for the background unconstrained fits. This difference is assigned as part of the systematic error.

Table 5 summarizes the different systematic errors for the three variables. The total system-

Sources of systematic errors	Variable		
	H_T	M_T	M
Energy scale uncertainty	8	8	8
Monte Carlo model	3	8	9
Interpolation bias	3	3	3
Background shape uncertainty	4	4	4
Total	10	12	13

Table 5: Breakdown of estimated systematic errors on the extracted masses of the top quark for the three variables.

Variable	m_t (GeV/c^2)	
	Background constrained	Background unconstrained
H_T	$178 \pm 21 \pm 10$	$170 \pm 18 \pm 10$
M_T	$182 \pm 21 \pm 12$	$171 \pm 18 \pm 12$
M	$169 \pm 20 \pm 13$	$163 \pm 16 \pm 13$

Table 6: The mass of the top quark extracted from the H_T, M_T and M distributions of the 34 lepton+jets $t\bar{t}$ candidate events. The first errors are statistical and the second errors are systematic.

atic errors derived by adding individual errors in quadrature are 10, 12 and 13 GeV/c^2 for the masses determined from the H_T, M_T and M distributions respectively. The top quark masses (with their statistical and systematic errors) extracted from the three variables are tabulated in Table 6. The central values of the masses are taken from the results of the fits using the HERWIG 5.7 program. The masses determined from the distributions of the three variables agree with each other for both background constrained and background unconstrained fits.

As discussed above, the distributions of the H_T, M_T and M variables are equally sensitive to the mass of the top quark. However, the systematic effects are not equal as shown in Table 5. Among the three variables, the M distribution is the most vulnerable to systematic uncertainties. Apart from its dependence on the transverse momentum spectrum of the top quark and the final state radiations, the distribution is also susceptible to the longitudinal momentum spectrum of the top quark and the initial state radiations. Between the H_T and M_T variables, it appears that both the HERWIG 5.7 and the ISAJET 7.13 programs model the H_T distribution better than the M_T distribution as indicated by the values of $-\ln\mathcal{L}$ from the fits. Also, the mass from the H_T distribution has a smaller systematic error as shown in the Table 6. Nevertheless, the extracted masses from the three distributions agree with each other within errors.

7 Summary

We have measured the mass of the top quark using the distributions of the three topological variables: the transverse momentum (H_T), the transverse mass (M_T) and the total mass (M) of the 34 lepton+jets $t\bar{t}$ candidate events. The top quark mass extracted from these variables are consistent and agree with that determined from the fit using kinematic constraints. In particular, the mass determined from the H_T distribution is $178 \pm 22(\text{stat}) \pm 10(\text{syst})$ GeV/c^2 for the background constrained fit and is $170 \pm 18(\text{stat}) \pm 10(\text{syst})$ GeV/c^2 for the background unconstrained fit. In addition, the fitted distributions describe the distributions of the candidate events well. This analysis complements the mass analysis of the kinematic fit and provides an independent measurement of the mass of the top quark.

References

[1] M. Pang, Ph.D. Thesis, Iowa State Univ., 1994, (Unpublished).
S. Snyder, Ph.D. Thesis, SUNY Stony Brook, 1995, (Unpublished).

[2] R. Partridge, talk at the Moriond conference, 1996.
M. Narain, talk at the La Thuile conference, 1996.

[3] HERWIG 5.7 Program:
G. Marchesini and B. Webber, Nucl. Phys. **B310** (1988) 461;
I.G. Knowles, Nucl. Phys. **B310** (1988) 571;
G. Marchesini *et al.*, Comp. Phys. Comm. **67** (1992) 465.

[4] ISAJET 7.13 7.13 Program:
F. Paige and S. Protopopescu, BNL Report No. BNL38034, 1986 (Unpublished).

[5] VECBOS Program:
F.A. Berends *et al.*, Nucl. Phys. **357**, 32 (1991).

[6] These numbers are from Frank Hsieh's mass analysis.